Rev. Adv. Mater. Sci. 53 (2018) 206-217

NEGATIVE MAGNETIZATION IN PEROVSKITE RTO_3 (R=RARE-EARTH, T=Cr/Mn)

Sanjay Biswas and Sudipta Pal

Department of Physics, University of Kalyani, Kalyani, Nadia, West Bengal, 741235, India

Received: October 24, 2017

Abstract. The present review presents a detail discussion of the phenomenon of magnetization reversal (or negative magnetization) phenomena. A variety of magnetically ordered systems shows negative magnetization. However, this negative magnetization in these materials does not arise due to diamagnetism. Here we have focused a special group of ceramic oxides namely RTO_3 (R=rare-earth, T=Cr/Mn). In these oxides sign of the magnetic moment reverses mainly due to negative exchange coupling among ferromagnetic/canted-antiferromagnetic and paramagnetic sublattices. Finally, the practical utilization of this type of materials is included in this review.

1. INTRODUCTION

The study of the rare-earth transitional metal (RTM) oxides with perovskite structure (with general formula ABO_3 where *A* and *B* denote the rare-earth and transitional metal respectively) is an interesting area of basic condensed matter physics research. Apart from the technological point of view, spectacular and unconventional magnetic ground states are observed in these compounds mainly due to the competing interactions of the internal degrees of freedom like spin, charge or orbital momentum. An enormous number of studies have been done to clarify the exchange interaction, nature of spin, charge or orbital ordering of the transition metal ions which changes the physical properties of these compounds. One of the interesting behavior in these RTM oxides is reversal of magnetization occurring in the antiferromagnetic phase.

When temperature dependent DC magnetization in a material turned to a negative value from a positive value the phenomenon is typically called magnetization reversal or negative magnetization. This negative magnetization (positive differential susceptibility) is different from a diamagnetic state (negative differential susceptibility) that occurs in the case of superconducting/diamagnetic materials. The magnetic moment of a magnet is aligned parallel to the applied magnetic field and the overall energy becomes lowest. The magnetic moment can be reversed by an appropriately large magnetic field in the reverse direction. But the magnetization reversal in response to a variation in temperature (in a small magnetic field) is rarer. Some ferrimagnetic compounds consisting of two or more types of antiferromagnetically ordered magnetic ions show this type of phenomena. An antiparallel arrangement among the canted AFM and PM sublattices belong to at different crystallographic sites may also show the negative magnetization. Usually, in such case, the paramagnetic atom practices an effective negative molecular field due to the adjacent ordered canted AFM sublattices. The observed net negative magnetization of such compounds can be estimated as Curie-Weiss type equation [1,2],

$$M = M_{TM} + \frac{C(H_{int} + H_{ext})}{(T - \theta_W)}, \qquad (1)$$

Corresponding author: Sudipta Pal, e-mail: sudipta.pal@rediffmail.com

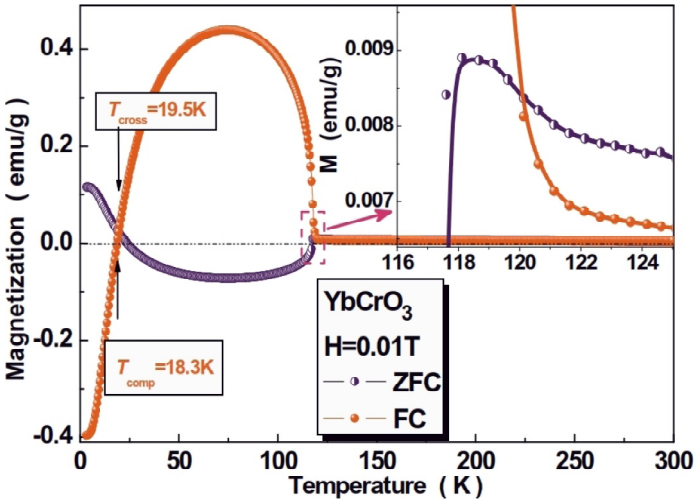

Fig. 1. ZFC and FC temperature dependent magnetization curve for $YbCrO_3$. The inset shows an magnifying part near T=120K. Reproduced from [5] with the permission of AIP Publishing.

where M_{TM} is the spontaneous magnetization of the transition metal ion sublattice, C is the Curie constant, H_{int} and H_{ext} are the internal (due to the transition metal ion sublattices ordering) and external magnetic fields, respectively.

Interestingly a large number of materials show this property. A good review has been also published recently on the phenomenon of negative magnetization [3]. The nature of magnetic properties with temperature shows no similarity in these materials. However, in the manganites and chromites ($RMnO_3$ or $RCrO_3$) the magnetic properties are almost comparable. In view of this phenomenon, we have tried to cover this special group of materials in this review. The effect of doping on the magnetization property has been discussed elaborately.

2. NATURE OF NEGATIVE MAGNETIZATION AND THEORETICAL ANALYSIS

2.1. Chromites compounds

2.1.1. $RCrO_3$

Rare earth chromium oxides $RCrO_3$ (R, lanthanides) have an orthorhombic perovskite structure at room temperature. The $RCrO_3$ compounds in general have *Pbnm* space group. The lattice parameters a and c decreases while b increase with the decrease of ionic radii of the R^{3+} ion. *Shtrikman et. al.* [4] reported that the strong anisotropic exchange interaction between the Cr^{3+} and Yb^{3+} spins in $YbCrO_3$ can induce various kinds of cooperative excitations. The Cr spins in $YbCrO_3$ are anti-ferromagnetically ordered below T_N, with a weak ferromagnetic moment. The magnetization curve in $YbCrO_3$ [5], exhibits an antiferromagnetic like transition around T_N =118K with lowering of temperature. On further lowering of temperature in the field cooled (FC) mode, the magnetization increases and shows a maximum value at 75K and then crossing the zero field cooled (ZFC) magnetization value (Fig. 1). In this system, the Yb^{3+} ion has only one 4*f* hole, and widely spread the 4*f* orbital, leading to a 3*d*–4*f* exchange interaction. Due to the antiferromagnetic interaction between Yb^{3+} and the canted Cr^{3+} moments, the Yb^{3+} magnetic moments are polarized antiparallel with respect to ferromagnetic chromium (Cr^{3+}) spins. As temperature decreases, the Yb^{3+} moments are aligned in the internal field of the chromium moments. As soon as the polarizations of the Yb^{3+} moments go beyond the ferromagnetic component, the total magnetization shows negative magnetization. Reversal phenomenon is also seen in $YbCrO_3$ nanocrystals [6].

In the case of perovskite chromate $GdCrO_3$ [7] (space group *Pnma*) it was proposed that the canted-antiferromagnetic order of Cr^{3+} produces an internal field at the Gd^{3+} site, whose direction is opposite to the net Cr^{3+} moment. Temperature dependent magnetization curves measured in a field-cooled cooling (FCC) mode are shown in Fig. 2 from Yoshii *et al.* [1]. This sample shows the canted-antiferromagnetic order of Cr^{3+} moments with a Neel temperature (T_N ~170K). This negative magnetization behaviour is understood by considering the paramagnetic Gd moments are reverse to that of canted Cr^{3+} moments. But in zero field cooling (ZFC) and field-cooled heating (FCH) sample does not show negative magnetization. There is report of Raman

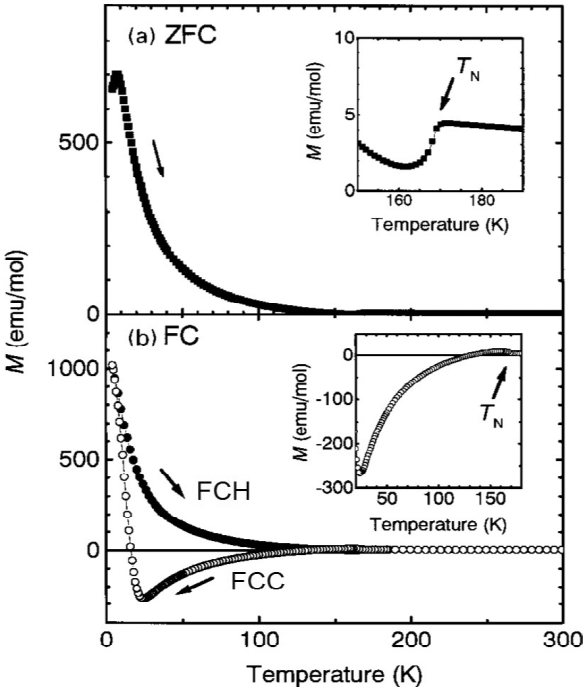

Fig. 2. (a) ZFC and (b) FC temperature dependent magnetization curve (M T) curves for GdCrO3 with an applied Field of *H*=100 Oe. Reproduced from [1] with the permission from Elsevier.

study on $GdCrO_3$ [8] however it does not shed any light on the negative magnetization property. Single crystal [9] and nanoparticles [10] also shows similar negative magnetization phenomenon. The behaviour of negative magnetization is observed for nanocrystalline phase pure $CeCrO_3$ [11] and for single phase $CeCrO_3$ [12]. Similarly, single phase $HoCrO_3$ [13,14] also show the negative magnetization and the transition temperature is different. In $TmCrO_3$ [15], the FCC and ZFC curves deviation are recognized to the magnetic ordering as shown in Fig. 3. The FCC magnetization shows a wide-ranging peak at ~70K and decreases again with temperature and leads to a compensation temperature (T_{comp}) of ~28K. Under the compensation temperature, the polarity of magnetization becomes negative. The magnetization becomes the minimum value at ~10K and sharply upturns at this temperature. This temperature is ascribed to a spin reorientation. $SmCrO_3$ [16,17] shows interesting magnetization reversal properties. However this property is not observed in (La/Pr)CrO_3 [18].

2.1.2. Mixed rare earth chromites

Large changes in the magnetic properties are observed when the rare earth atom is substituted by other due to the change in the magnetic moment and ionic radii of the rare earth ion. *Yoshii et. al.* [19] found that the mixed lanthanide orthochromate $La_{0.5}Pr_{0.5}CrO_3$ exhibits large negative magnetization when its magnetization (*M*) vs temperature (*T*) curves are measured in FC (Field-cooled) mode as shown in Fig. 4. This sample displays a canted-antiferromagnetic transition at ~261K and a peak with a positive value at~220K. With decreasing temperature *M* decreases and shows a zero value (*M*=0) around 163K. Below this temperature magnetization value shows negative. It was reported that $La_{1-x}Pr_xCrO_3$ [20,21] show negative magnetization with other Pr concentration also. In low applied magnetic fields, the samples display distinct negative magnetization below the compensation temperatures. Neutron diffraction data also exhibited the reality of G_y-type (G_z for *Pbnm*) antiferromagnetic

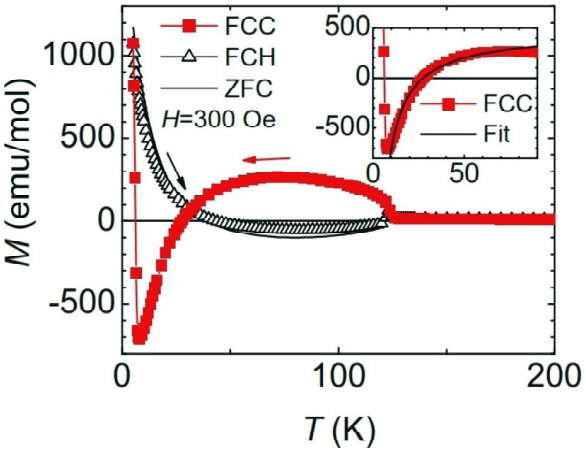

Fig. 3. Temperature dependent magnetization curves of $TmCrO_3$. The inset shows the Curie–Weiss fit of the FCC data. Reproduced from [15] with permission from Springer.

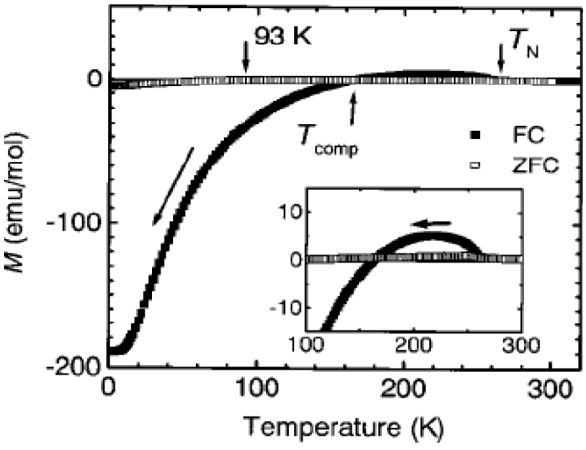

Fig. 4. FC and ZFC temperature dependent magnetization curve for $La_{0.5}Pr_{0.5}CrO_3$. The inset shows the temperature area above 100K for FC curve. Reproduced from [19] with permission from Elsevier.

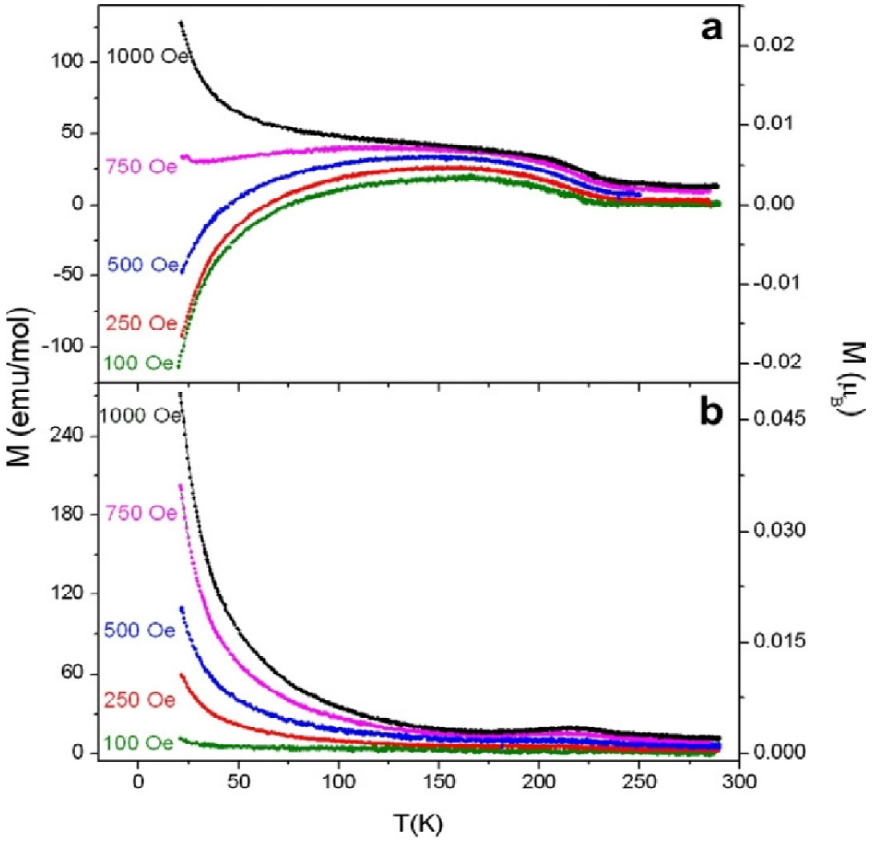

Fig. 5. Temperature dependent magnetization curves recorded under different external magnetic fields in (a) FC mode and (b) ZFC mode. Reproduced from [26] with permission from Elsevier.

order of Cr^{3+}. The negative magnetization in these samples is due to the antiparallel coupling of the Pr^{3+} moments and the canted Cr^{3+} moments.

The reversal of magnetization in low applied field in $La_{0.75}Nd_{0.25}CrO_3$ [22] is due to the antiferromagnetic coupling between Nd^{3+} and the canted Cr^{3+} moments. The Nd^{3+} moments are more and more aligned in the internal field of the chromium moments as temperature decreases. When the magnetic moments of the Nd^{3+} exceed the ferromagnetic component of the Cr^{3+} sublattice shows a negative magnetization. The behaviour of the magnetization is also observed in $La_{1-x}Ce_xCrO_3$ [23] and $La_{0.2}Ce_{0.8}CrO_3$ [24,25] compounds in nanocrystalline form where an AFM interaction between the Cr^{3+} and Ce^{3+} moments is present. In $La_{0.5}Gd_{0.5}CrO_3$ [26] and $La_{0.1}Gd_{0.9}CrO_3$ [27] the negative magnetization can be explained by considering Gd and Cr magnetic sublattices aligned antiparallel each other. Temperature dependent magnetization curves of $La_{0.5}Gd_{0.5}CrO_3$ recorded in FC mode under different applied magnetic fields ranging from 100 Oe to 1000 Oe has been shown in Fig. 5. The compensation temperature (T_{comp}) decreases with increasing field until an applied field of 500 Oe is reached. No magnetization reversal occurs for higher applied magnetic fields indicating that they prevent the opposite alignment of the rare earth moments. Neutron diffraction in $Y_{0.9}Pr_{0.1}CrO_3$ [28] shows the co-existence of magnetic phases and domains at low temperature depend sensitively on the external cooling field. The G_zF_x ($PrCrO_3$) ordering is dominant when the cooling field is lower than 15 Oe, while for cooling fields higher than 100 Oe, the G_xF_z ($YCrO_3$) ordering is dominant. The effect of doping on the magnetization reversal property is observed in $Gd_{0.5}Dy_{0.5}CrO_3$ [29], $Y_{0.9}R_{0.1}Fe_{0.5}Cr_{0.5}O_3$ (R = Eu and Nd) [30] $Y_{1-x}Ho_xFe_{0.5}Cr_{0.5}O_3$ [31,32].

2.1.3. Divalent or trivalent doped rare earth chromites

In $Gd_{1-x}Ca_xCrO_3$ (x=0.0-0.3) [2], the temperature dependent DC magnetization characteristic reveal exciting results as shown in Fig. 6. The negative magnetization is absent for all the samples in ZFC mode. In the FCC mode below the Néel temperature, the magnetization first rises and then rapidly decreases to a negative value for all the samples. In these samples M_{Cr} and M_{Gd} are anti-parallel to each other. With lowering of temperature, the disordered

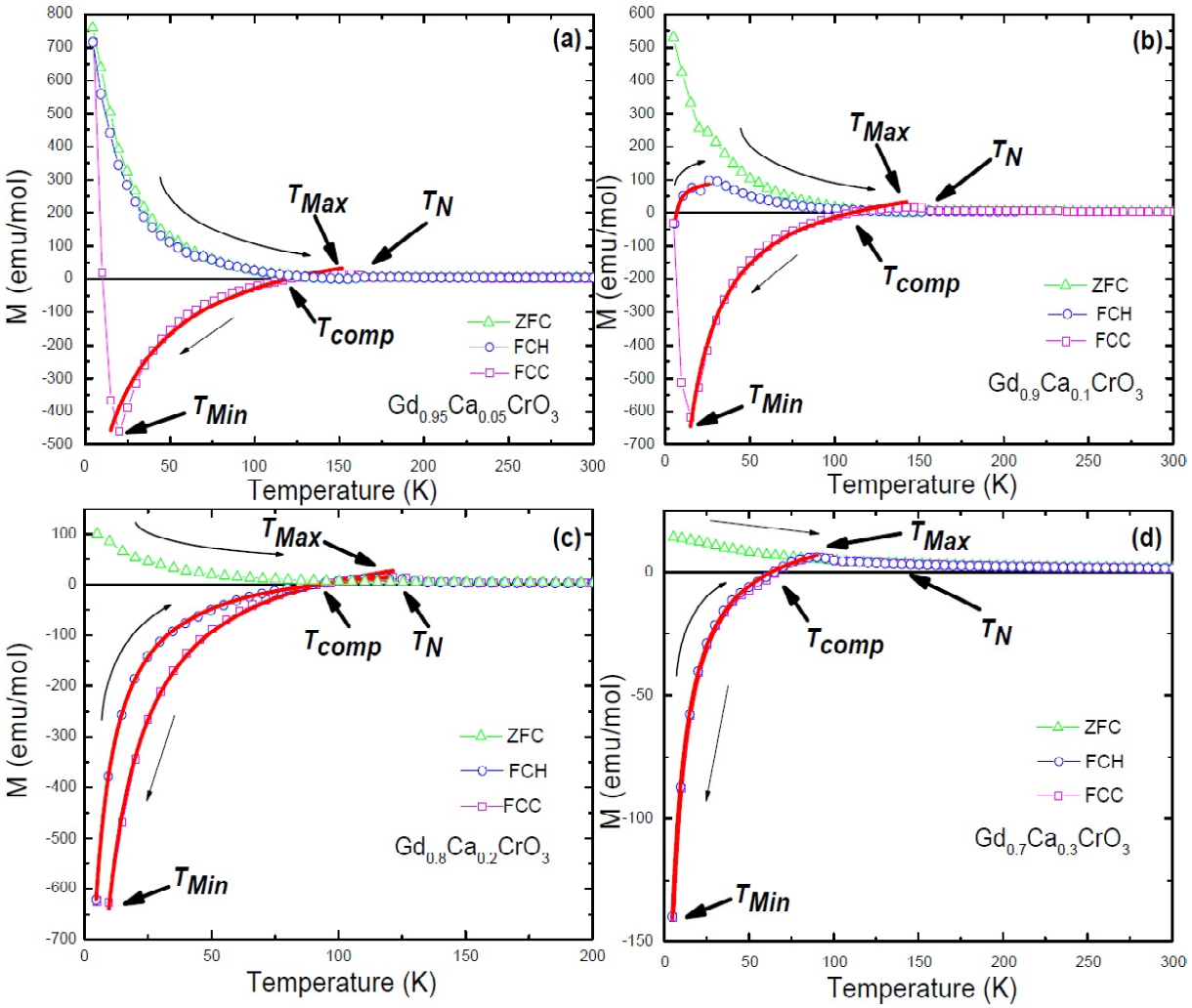

Fig. 6. DC temperature dependent magnetization curve in ZFC, FCC, FCH mode for (a) $Gd_{0.95}Ca_{0.05}CrO_3$, (b) $Gd_{0.9}Ca_{0.1}CrO_3$, (c) $Gd_{0.8}Ca_{0.2}CrO_3$, (d) $Gd_{0.7}Ca_{0.3}CrO_3$. Solid line shows fitting using Eq. (1) of *M-T* data recorded in a magnetic field 100 Oe. Reproduced from [2] with permission from Elsevier.

M_{Gd} ions begin to polarize in contradiction of the canted field of M_{Cr} moments. The overall magnetization of the compound becomes $M = M_{Cr} - M_{Gd}$. The value of M_{Gd} rises significantly faster than M_{Cr} below T_{max}. At the T_{comp}, M_{Cr} and M_{Gd} become an equal value and the total net magnetization becomes zero. Below the T_{comp}, the overall magnetization converts into a negative value. The red solid lines in Fig. 6 show the fitting to the *M–T* curve using Eq. (1). Ca doping at Gd site changes the magnetization properties. Similarly, reversal phenomenon is also changes by doping of Bi in $Sm_{0.9}Bi_{0.1}CrO_3$ [33] and doping of Y in $Gd_{1-x}Y_xCrO_3$ [34].

2.1.4. Cr replaced by other transition metal

Interesting changes in the magnetization reversal properties are observed in the polycrystalline samples $LaCr_{0.85}Mn_{0.15}O_3$ [35], $LaCr_{0.8}Mn_{0.2}O_3$ [36], $LaCr_{1-x}Fe_xO_3$ [37], $SmCr_{0.8}Fe_{0.2}O_3$ [38], $NdCr_{1-x}Fe_xO_3$ [39], $NdCr_{1-x}Mn_xO_3$ [40]. The effect of Mn doping at Cr site in the magnetization properties for the sample $SmCr_{0.9}Mn_{0.1}O_3$ [41] has been shown in Fig. 7. With a small doping of magnetic ions Mn^{3+} at Cr^{3+} sites, temperature-induced negative magnetization is observed. The reason for the magnetization reversal is attributed to the competitive interaction between Cr-rich clusters and Cr–Mn ordered clusters where the net moments of the two clusters oriented in opposite direction. In the Fe doped compounds the magnetization reversal is explained by taking considering the competition between the canted FM component of Cr^{3+} ions and the paramagnetic moments of Nd^{3+} and Fe^{3+} in negative internal field. Similar changes has been observed in $SmCr_{1-x}Mn_xO_3$ [42] $SmCr_{0.85}Mn_{0.15}O_3$ [43], $EuCr_{0.85}Mn_{0.15}O_3$ [44], $YbCr_{1-x}Ru_xO_3$ [45],

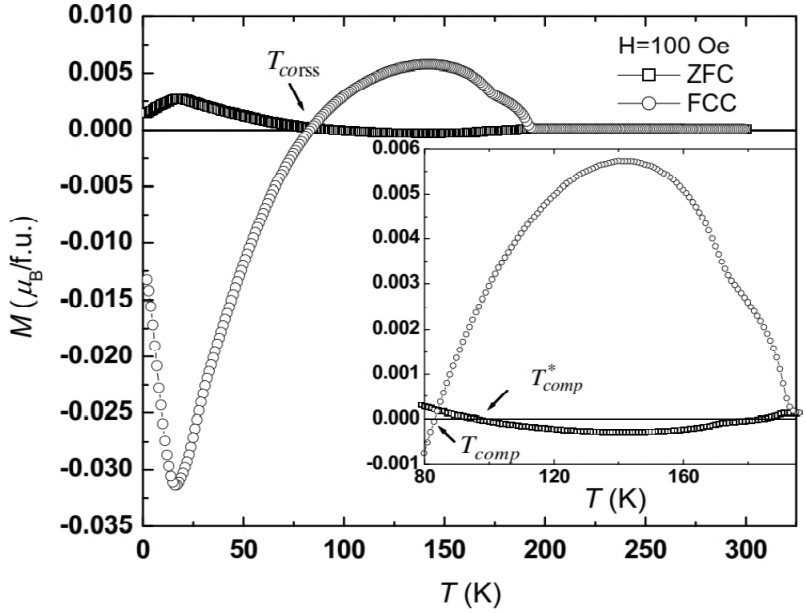

Fig. 7. Temperature dependent magnetization curves at an applied field of 100 Oe under ZFC and FCC for $SmCr_{0.9}Mn_{0.1}O_3$. The inset shows an magnifying part. Reproduced from [41] with permission from Springer.

$RFe_{0.5}Cr_{0.5}O_3$ [46,47], $NdFe_{0.5}Cr_{0.5}O_3$ [48] and $YCr_{1-x}Mn_xO_3$ ($0.15 \le x \le 0.4$) [49] and $GdCr_{1-x}Mn_xO_3$ [50]. Magnetization reversal in these compounds is described based on the competition among Cr^{3+}–Cr^{3+}, Mn^{3+}–Mn^{3+} and Cr^{3+}–Mn^{3+} interactions.

2.2. Manganite compounds

2.2.1. $RMnO_3$

In the case of $RMnO_3$ compounds very few shows negative magnetization. Among them, $NdMnO_{3+\delta}$ [51] shows magnetization reversal phenomenon shown in Fig. 8. The results specify that at sufficiently low temperature the Nd moments were polarized by Nd–Mn interaction in a parallel fashion, antiparallel to the Mn net moment. As temperature decreases, the Nd^{3+} moments are more and more aligned in the internal field of the Mn moments shows a negative magnetization at the lowest temperatures, when the polarization of the Nd^{3+} moments surpasses the ferromagnetic component of the Mn^{3+} sublattice. Similarly $NdMnO_3$ [52] also show this interesting phenomenon. *Jung et. al.* observed in $SmMnO_3$ [53] temperature-induced magnetization reversal due to keen competition between ferrimagnetically coupled polarized Sm and canted Mn moments.

2.2.2. Mixed rare earth manganites

Zhang et. al. reported that electron-doped $Nd_{1-x}Ce_xMnO_3$ [54] also show the negative magnetization and these results are explained successfully in terms of Weiss's molecular field theory and Neel's two-sublattice model. The single crystal samples of $La_{1-x}Gd_xMnO_3$ [55] show negative magnetization in the FCC measurements. The magnetization reversal in this samples effects from the complex interaction of the 3*d*–4*f* magnetism. The Gd spins and the net FM moment of Mn spins are polarized antiparallel. The net magnetization of these materials can be predictable by considering the discrete contributions from the Gd and Mn sites.

Temperature dependent DC magnetization of $Pr_{1-x}Gd_xMnO_3$ (x=0.3, 0.5, 0.7) [56-58] show the reversal of magnetization in ZFC and FC mode (Fig.

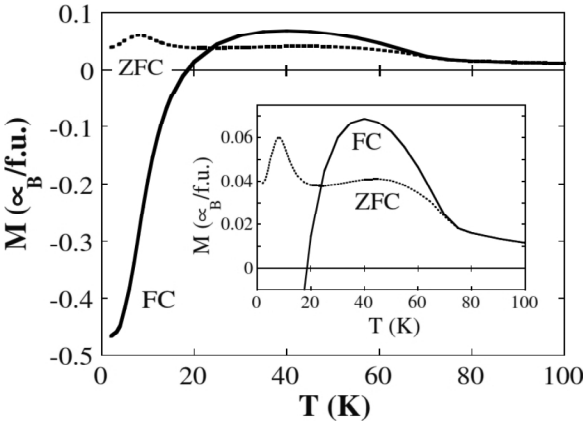

Fig. 8. FC (solid line) and ZFC (dotted line) $NdMnO_{3.11}$ magnetization with an applied field H=1 kOe. Reproduced from [51] with permission from Elsevier.

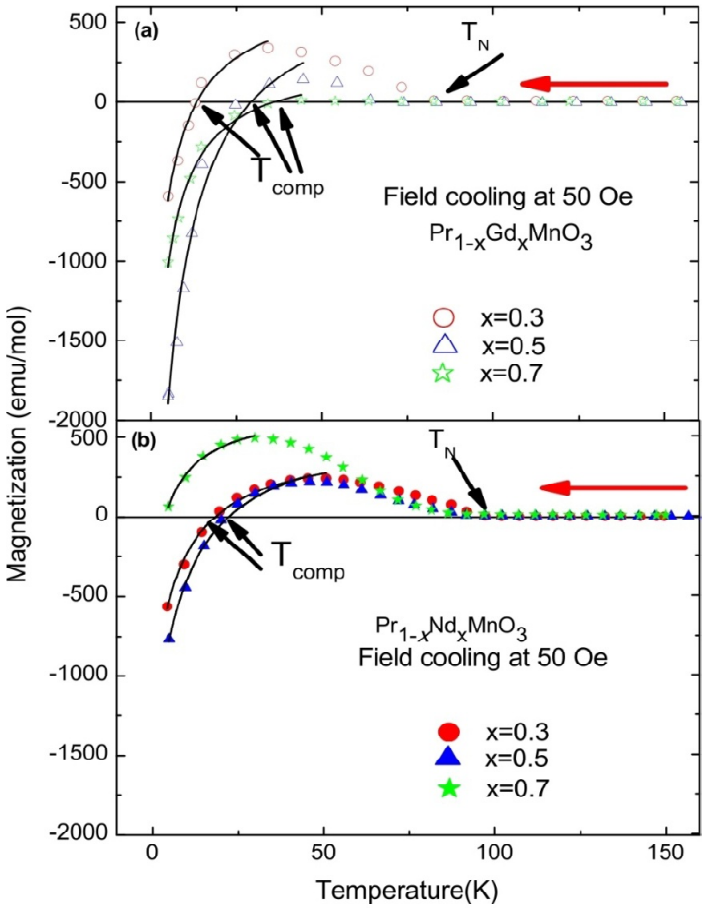

Fig. 9. DC temperature dependent magnetization curve in FC mode of (a) $Pr_{1-x}Gd_xMnO_3$ (x=0.3, 0.5, 0.7) and (b) $Pr_{1-x}Nd_xMnO_3$ (x=0.3, 0.5, 0.7). Solid line shows fitting using Eq. (1) of M–T data recorded under 50 Oe. Reproduced from [57] with permission from IOP publishing.

9a). It is interesting that neither $PrMnO_3$ nor $GdMnO_3$ does not show negative magnetization. However this property is observed in their solid solution. The red solid lines in Fig. 9a show the fitting to the M–T curve using Eq. (1).The negative magnetization of $Pr_{1-x}Nd_xMnO_3$ (x=0.3, 0.5, 0.7) [56, 57] has shown in Fig. 9b. In the sample x=0.3 and 0.5, the FC magnetization turns into negative value below temperature 18K and 22K respectively. The negative magnetization may have a connection with the weakening of anisotropy around Pr^{3+}, arising from the replacement of Nd^{3+}. With the dropping of temperatures, the Pr and Nd spins begin to polarize opposite to the exchange field of the manganese moments and finally, yielding a negative magnetization, when the polarization of the |Pr+Nd| spins go beyond the FM component of the Mn moments. The M–T curve follows Eq. (1) shown by the red solid lines in Fig. 9b. Solid solution of other manganite like $(Nd_{1-x}Gd_x)_{0.55}Sr_{0.45}MnO_3$ [59] also show reversal of magnetization phenomena.

2.2.3. Divalent doped rare earth manganites

Magnetization reversal in the manganite is first reported by *Nordman et. al.* in the thin-films of compound $Dy_{0.67}Ca_{0.30}MnO_{3+d}$ [60]. At low temperature, it exhibits ferrimagnetic nature. With lowering temperature, the magnetization of the sublattice is antiparallel with the field and shows negative magnetization. $Dy_{1-x}Ca_xMnO_3$ show in the ZFC/FC magnetization cycles a ferrimagnetic-like nature [61], in which negatively-polarized dysprosium moments behave as free spins (T > Neel temperature (T_N)) under the internal field of the ordered Mn sublattice. The local field at Dy site depends on the negative exchange interaction between both sublattices. The compounds show negative magnetization when the magnetic moment of the Dy sublattice superior to the ferromagnetic network. The solid solution of $Dy_{1-x}Ca_xMnO_3$ [62] shows negative (AF) interaction between both sub-lattices, in which the Dy moments align parallel, but in opposite direction to the inter-

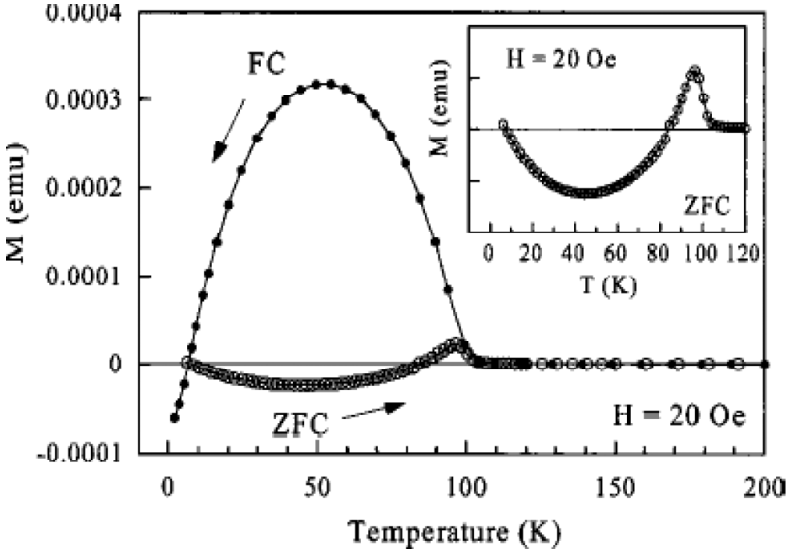

Fig. 10. Temperature dependent magnetization curves for the GCMO thin film under ZFC and FC conditions. The inset shows an magnifying part of figure. Reproduced from [65] with permission from WILEY-VCH Verlag GmbH & Co. KGaA.

nal field formed by the Mn network. At sufficiently low temperatures, the Dy sublattice contribution surpasses the contribution of the Mn sublattice, producing a reversal of the sign of the magnetization, as observed in the ferrimagnetic systems.

The bulk, single crystal, and metal-organic chemical-vapor deposition thin-film samples of $Gd_{0.67}Ca_{0.33}MnO_3$ [63] shows ferrimagnetic nature and at low temperature shows negative magnetization. A molecular field model with a ferromagnetic manganese sublattice antiparallel to the Gd sublattice qualitatively explains the magnetic properties. The solid solution of $Gd_{1-x}Ca_xMnO_3$ [64] shows ferrimagnetic-like properties. Results are clarified in terms of two interacting magnetic sublattices. The larger magnetic moment of the Gd sublattice than the Mn-based ferromagnetic network leads to negative magnetization. *Ma et. al.* reported about the negative magnetization for the epitaxial thin film of $Gd_{0.67}Ca_{0.33}MnO_3$ [65] as shown in Fig. 10. The negative *f-d* exchange interaction creates the Gd sublattice aligned antiparallel to such local field. If the anti-aligned sublattice magnetization rises more quickly below the compensation temperature the magnetization becomes negative. When the applied magnetic field is high enough, it overcomes the internal field produced by the Mn sublattice. Gd ions in the sample remain parallel to the externally applied field and suppressed the negative magnetization phenomenon. Even a small amount of divalent doping (about 10%) in $Gd_{0.9}Ca_{0.1}MnO_3$ [66, 67] shows the reversal of magnetization phenomenon.

The changes in the negative magnetization properties due to Sr doping in the single crystal $Sm_{1-x}Sr_xMnO_3$ [68] shows as shown in Fig. 11. An antiparallel alignment of the Mn moment and Sm moment driven by Sm–Mn exchange interaction effects the magnetization property. In other rare earth manganites like $Gd_{1-x}Sr_xMnO_3$ [69, 70], $Dy_{0.6}Sr_{0.4}MnO_3$ [71], and $Tb_{0.7}Sr_{0.3}MnO_3$ [72] reversal of magnetization phenomena has been studied with Sr doping.

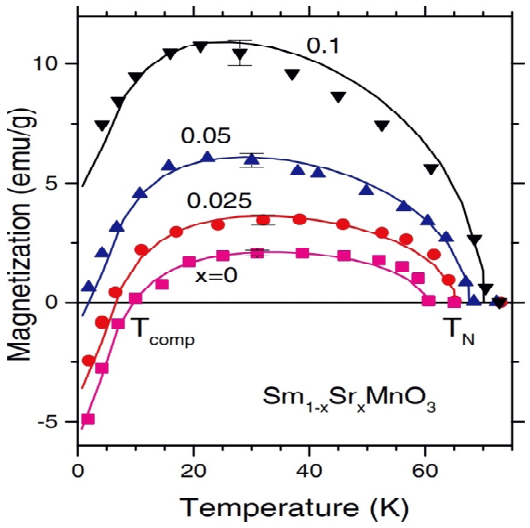

Fig. 11. Temperature dependent spontaneous magnetization for $Sm_{1-x}Sr_xMnO_3$ crystals, experiment (points) and theory (solid lines). Reproduced from [68] with permission from AIP Publishing.

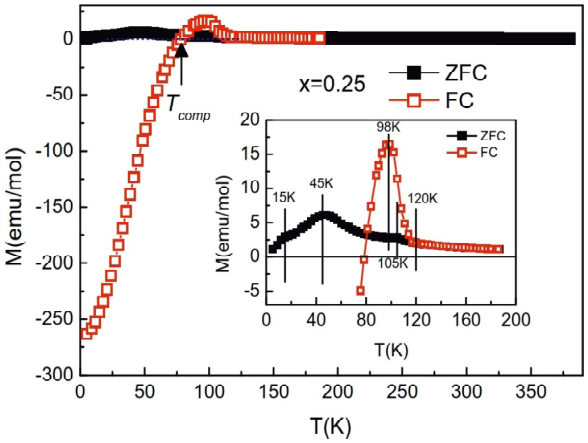

Fig. 12. Temperature dependent magnetization curves for $Bi_{0.3}Ca_{0.7}Mn_{0.75}Cr_{0.25}O_3$ under ZFC and FC modes respectively. The inset is the enlarged part of *M*(*T*) curves. Reproduced from [75] with permission from Elsevier.

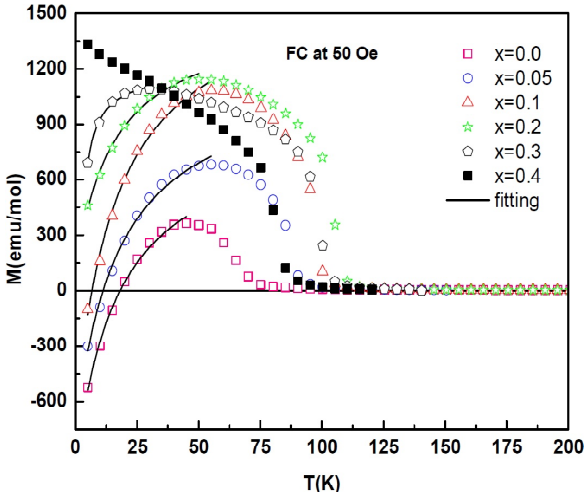

Fig. 13. Temperature dependent magnetization curves for $Gd_{0.7}Ca_{0.3}Mn_{1-x}Cr_xO_3$ (*x*=0.0, 0.05, 0.1, 0.2, 0.3, 0.4) in FC mode. Solid line in shows Curie-Weiss type fitting using Eq. (1) of *M*-*T* data. Reproduced from [76] with permission from Elsevier.

2.2.4. Mn replaced by other transition metal

Fractional replacement of Mn by another transition metal *Me*=Co, Ni in the rare-earth (RE) manganites $REMe_xMn_{1-x}O_3$ [73,74] results interesting changes in the simultaneous existence of Mn^{3+} and Mn^{4+}. The sample $Gd(Me,Mn)O_3$ [73] in which the manganese sublattice has been partially doped by transition metal elements leaving the gadolinium network intact. The reversal of magnetization can be clarified by assuming a negative exchange interaction between the [Mn+*Me*] and the Gd moments. At the compensation temperature both the magnetic moments reach the same absolute value and below this compensation temperature, the total magnetization turns into a negative value. The rare earth sublattice has its specific properties and can interact with the local field imposed by the ferromagnetic network. Its alignment differs depending on the rare earth nature, accepting most usually a parallel direction with respect to the field, but in other cases, it may align in an opposite direction.

It was found that the polycrystalline compound $Bi_{0.3}Ca_{0.7}Mn_{0.75}Cr_{0.25}O_3$ [75] shows a negative magnetization in the FC magnetization curves as shown in Fig. 12. The source of the negative magnetization is the temperature dependence of the antiparallel alignment of Cr^{3+} and the canted $Mn^{3+/4+}$ moments. The Cr^{3+} ionic moments are polarized opposite to the ordered Mn moments. So, increase in the Cr^{3+} ionic moments aligned opposite to the applied magnetic field causes the reversal of magnetization in this compound.

In the field cooled (FC) mode, the negative magnetization observed for the compounds $Gd_{0.7}Ca_{0.3}Mn_{1-x}Cr_xO_3$ (*x*=0.0–0.5) [76] in the external applied field *H* = 50 Oe as shown in Fig. 13. The red solid lines in Fig. 13 show the fitting to the *M*–*T* curve using Eq. (1). The investigation of magnetization measurement results evidently indicates the presence of two components in the magnetic ordering, which is suggested to come from the contribution of opposite alignment of Gd ions with respect to the |Mn+Cr|. Therefore, the net magnetization of the system is $M_s = M_{Mn+Cr} - M_{Gd}$. Below T_{comp}, M_{Gd} is much larger than M_{Mn+Cr}. Since the coercivity of the system is considerably larger than the applied magnetic field, the magnetic domains are sealed in the original direction and M_{Gd} remains antiparallel to the applied field. Therefore the net magnetization should be a negative value. $Gd_{0.7}Ca_{0.3}Mn_{1-x}Ru_xO_3$ [77] and $GdMn_{1-x}Cr_xO_3$ [78] are also show reversal of magnetization phenomena. The magnetization reversal phenomena in $YFe_{1-x}Mn_xO_3$ [79] or $NdMn_{1-x}Fe_xO_{3+\delta}$ [80] has be explained by the random occupation of magnetic ions and diverse magnetic interactions, Fe-O-Fe, Fe-O-Mn, and Mn-O-Mn.

3. APPLICATIONS OF NEGATIVE MAGNETIZATION IN MANGANITES AND CHROMITES

Applications of the rare earth transition metal oxides are manifold in the industrial, commercial and military worlds depending on their multifunctional properties. Specifically the phenomenon of negative magnetization can be considered in various prac-

tical applications/ devices. The temperature induced magnetization reversal is potential for application in contemporary magnetic memories, e.g., thermally assisted magnetic random access memory (TAMRAM). In a negative magnetization material sign reversal of the exchange bias is observed which might be utilized as an alternative for the magnetization switching in magnetic memories. Temperature dependent sign-reversal of magnetization without reversing the applied magnetic field might be used as magnetic switching. Magnetocaloric effect or the magnetic entropy change under varying temperature and magnetic field in these materials can also have practical applications in magnetic refrigeration technology.

4. CONCLUSIONS

The experimental and theoretical characteristics of the reversal of magnetization are discussed with up to date literatures. The negative magnetization phenomenon in these perovskite rare earth transition-metal (Mn, Cr) oxides occurs mainly due to two or more magnetic sublattice showing different temperature dependent magnetization properties. Large magnetic moment of the rare earth ion and weak ferromagnetism in these oxides might result in negative magnetization. It is interesting to see that in all compounds the typical behavior occurs at very low external magnetic field. We have also included the utilization of these types of rare earth transition metal oxides. This review would also motivate researchers to produce new magnetic compounds that show a negative magnetization phenomenon near room temperature. So, these materials could be used for practical applications.

ACKNOWLEDGEMENTS

This work was partially supported by DST-FIST Govt. of India.

REFERENCES

[1] K. Yoshii //*J. Solid State Chem.* **159** (2001) 204.
[2] S. Biswas and S. Pal // *Ceramics International* **41** (2015) 14712.
[3] A. Kumar and S.M. Yusuf // *Physics Reports* **556** (2015) 1.
[4] S. Shtrikman, B.M. Wanklyn and I. Yaeger // *Int. J. Magn.* **1** (1971) 327.
[5] Y. Su, J. Zhang, Z. Feng, L. Li, B. Li, Y. Zhou, Z. Chen and S. Cao // *J. Appl. Phys.* **108** (2010) 013905.
[6] P. Gupta and P. Poddar // *Inorg. Chem.* **54** (2015) 9509.
[7] A.H. Cooke, D.M. Martin and M.R. Wells // *J. Phys. C: Solid State Phys.* **7** (1974) 3133.
[8] A. Jaiswal, R. Das, K. Vivekanand, T. Maity, P.M. Abraham, S. Adyanthaya and P. Poddar // *J. Appl. Phys.* **107** (2010) 013912.
[9] L.H. Yin, J. Yang, X.C. Kan, W.H. Song, J.M. Dai and Y.P. Sun // *Journal of Applied Physics* **117** (2015) 133901.
[10] S. Mahana, U. Manju, and D. Topwal // *AIP Conference Proceedings* **1832** (2017) 130046.
[11] R. Shukla, A.K. Bera, S.M. Yusuf, S.K. Deshpande, A.K. Tyagi, W. Hermes, M. Eul and R. Pöttgen // *J. Phys. Chem. C* **113** (2009) 12663.
[12] Y. Cao, S. Cao, W. Ren, Z. Feng, S. Yuan, B. Kang, B. Lu and J. Zhang // *Applied Physics Letters* **104** (2014) 232405.
[13] Y.L. Su, J.C. Zhang, L. Li, Z.J. Feng, B.Z. Li, Y. Zhou and S.X. Cao // *Ferroelectrics* **410** (2010) 102.
[14] Y. Su, J. Zhang, Z. Feng, Z. Li, Y. Shen and S. Cao // *J. Rare Earth.* **29** (2011) 1060.
[15] K. Yoshii // *Mater. Res. Bull.* **47** (2012) 3243.
[16] S. Huang, G. Zerihun, Z. Tian, S. Yuan, G. Gong, C. Yin and L. Wang // *Ceramics International* **40** (2014) 13937.
[17] P. Gupta, R. Bhargava and P. Poddar // *J. Phys. D: Appl. Phys.* **48** (2015) 025004 (10pp).
[18] K. Yoshii, N. Ikeda, Y. Shimojo and Y. Ishii // *Materials Chemistry and Physics* **190** (2017) 96.
[19] K. Yoshii and A. Nakamura // *J. Solid State Chem.* **155** (2000) 447.
[20] K. Yoshii, A. Nakamura, Y. Ishii and Y. Morii // *J. Solid State Chem.* **162** (2001) 84.
[21] K. Yoshii // *Appl. Phys. Lett.* **99** (2011) 142501.
[22] V.A. Khomchenko, I.O. Troyanchuk, R. Szymczak and H. Szymczak //*J. Mater. Sci.* **43** (2008) 5662.
[23] R. Shukla, J. Manjanna, A.K. Bera, S.M. Yusuf and A.K. Tyagi // *Inorg. Chem.* **48** (2009) 11691.
[24] P.K. Manna, S.M. Yusuf, R. Shukla and A.K. Tyagi // *Appl. Phys. Lett.* **96** (2010) 242508.
[25] P.K. Manna, S.M. Yusuf, M.D. Mukadam and J. Kohlbrecher // *Appl. Phys. A* **109** (2012) 385.

[26] N. Sharma, B.K. Srivastava, A. Krishnamurthy and A.K. Nigam // *Solid State Sci.* **12** (2010) 1464.
[27] N. Sharma, B.K. Srivastava, A. Krishnamurthy and A.K. Nigam // *J. Alloy. Compd.* **545** (2012) 50.
[28] D. Deng, J. Zheng, D. Yu, B. Wang, D. Sun, M. Avdeev, Z. Feng, C. Jing, B. Lu, W. Ren, S. Cao and J. Zhang // *Applied Physics Letters* **107** (2015) 102404.
[29] V.K. Tripathi and R. Nagarajan // *ACS Omega* **2** (2017) 2657.
[30] L.R. Shi, C.X. Wei and Z.C. Xia // *Journal of Alloys and Compounds* **698** (2017) 626.
[31] L.R. Shi, C.X. Wei, Z. Wang, L. Ju, T.S. Xu, T.X. Li, X.W. Yan and Z.C. Xia // *Journal of Magnetism and Magnetic Materials* **433** (2017) 104.
[32] L.R. Shi, Z.C. Xia, M. Wei, Z. Jin, C. Shang, J.W. Huang, B.R. Chen, Z.W. Ouyang, S. Huang and G.L. Xiao // *Ceramics International* **41** (2015) 13455.
[33] X.L. Qian, J. Kang, B. Lu, S.X. Cao and J.C. Zhang // *RSC Adv.* **6** (2016) 10677.
[34] B.B. Dash and S. Ravi // *Journal of Magnetism and Magnetic Materials* (2017) DOI: https://doi.org/10.1016/j.jmmm.2017.06.068
[35] T. Bora and S. Ravi // *J. Appl. Phys.* **114** (2013) 183902.
[36] T. Bora and S. Ravi // *Journal of Magnetism and Magnetic Materials* **358-359** (2014) 208.
[37] T. Bora and S. Ravi // *Journal of Applied Physics* **114** (2013) 033906.
[38] V.R. Bakshi, B.V. Prasad, N.R. Gade, F.C. Chou and S.B. Devarasetty // *AIP Conference Proceedings* **1591** (2014) 1735.
[39] T. Bora and S. Ravi // *Journal of Magnetism and Magnetic Materials* **386** (2015) 85.
[40] T. Bora and S. Ravi // *J Supercond Nov Magn* **28** (2015) 869.
[41] Y. Wu, J. Xu and Z. Xia //*J Low Temp Phys* **183** (2016) 14.
[42] B.B. Dash and S. Ravi // *Journal of Magnetism and Magnetic Materials* **405** (2016) 209.
[43] S. Kumar, I. Coondoo, M. Vasundhara, A.K. Patra, A.L. Kholkin, and N. Panwar // *J. Appl. Phys.* **121** (2017) 043907.
[44] S. Kumar, I. Coondoo, M. Vasundhara, V.S. Puli and N. Panwar // *Physica B: Condensed Matter* **519** (2017) 69.
[45] B. Dalal, B. Sarkar, V.D. Ashok and S.K. De // *J. Phys.: Condens. Matter* **28** (2016) 426001 (14pp).
[46] L.H. Yin, J. Yang, P. Tong, X. Luo, W.H. Song, J.M. Dai, X.B. Zhu and Y.P. Sun // *Appl. Phys. Lett.* **110** (2017) 192904.
[47] F. Pomiro, R.D. Sanchez, G. Cuello, A. Maignan, C. Martin and R.E. Carbonio // *Phys. Rev. B* **94** (2016) 134402.
[48] M.P. Sharannia, S. De, R. Singh, A. Das, R. Nirmala and P.N. Santhosh // *Journal of Magnetism and Magnetic Materials* **430** (2017) 109.
[49] C.L. Li, S. Huang, X.X. Li, C.M. Zhu, G. Zerihun, C.Y. Yin, C.L. Lu and S.L. Yuan // *Journal of Magnetism and Magnetic Materials* **432** (2017) 77.
[50] B.B. Dash and S. Ravi // *Journal of Magnetism and Magnetic Materials* **429** (2017) 281.
[51] F. Bartolome, J. Bartolome and J. Campo // *Physica B* **312–313** (2002) 769.
[52] A. Kumar, S.M. Yusuf and C. Ritter // *Phys. Rev. B* **96** (2017) 014427.
[53] J.S. Jung, A. Iyama, H. Nakamura, M. Mizumaki, N. Kawamura, Y. Wakabayashi and T. Kimura // *Phys. Rev. B* **82** (2010) 212403.
[54] S. Zhang, L. Luan, S. Tan and Y. Zhang // *Appl. Phys. Lett.* **84 (**2004) 3100.
[55] J. Hemberger, S. Lobina, H.A. Krug von Nidda, N. Tristan, V.Y. Ivanov, A.A. Mukhin, A.M. Balbashov and A. Loidl // *Phys. Rev. B* **70** (2004) 024414.
[56] S. Biswas, M.H. Khan and S. Pal // *Bull. Mater. Sci.* **37** (2014) 809.
[57] S. Biswas and S. Pal // *Phys. Scr.* **90** (2015) 065805 (5pp).
[58] S. Biswas, S. Pal and E. Bose // *Indian Journal Physics* **88** (2014) 1045.
[59] R. Kamel, A. Tozri, E. Dhahri, E.K. Hlil and L. Bessais // *Journal of Magnetism and Magnetic Materials* **426** (2017) 757.
[60] C.A. Nordman, V.S. Achutharaman, V.A. Vas'ko, P.A. Kraus, A.R. Ruosi, A.M. Kadin and A.M. Goldman // *Phys. Rev. B* **54** (1996) 9023.
[61] M. Mouallem-Bahout, O. Peńa, D. Gutierrez, P. Duran and C. Moure // *Solid State Commun.* **122** (2002) 561.
[62] O. Peńa, M. Bahout, D. Gutierrez, P. Duran and C. Moure // *Solid State Sci.* **5** (2003) 1217.

[63] G.J. Snyder, C.H. Booth, F. Bridges, R. Hiskes, S. DiCarolis, M.R. Beasley and T.H. Geballe // *Phys. Rev. B* **55** (1997) 6453.
[64] O. Peña, M. Bahout, K. Ghanimi, P. Duran, D. Gutierrez and C. Moure // *J. Mater. Chem.* **12** (2002) 2480.
[65] Y. Ma, M. Guilloux-Viry, P. Barahona, O. Pena and C. Moure // *Appl. Phys. Lett.* **86** (2005) 062506.
[66] S.K. Estemirova, V.F. Balakirev, A.M. Yankin, V.Y. Mitrofanov, S.A. Uporov, V.M. Kozin and T.I. Filinkova // *Glass Physics and Chemistry* **41** (2015) 224.
[67] A. Beiranvand, J. Tikkanen, H. Huhtinen and P. Paturi // *Journal of Alloys and Compounds* **720** (2017) 126.
[68] V.Y. Ivanov, A.A. Mukhin, A.S. Prokhorov and A.M. Balbashov // *Phys. Status Solidi B* **236** (2003) 445.
[69] Z. Yingnan, L. Junjia, Z. Ziqing, L. Fuyang, Z. Xudong and L. Xiaoyang // *Chem. Res. Chin. Univ.* **31** (2015) 699.
[70] B.S. Nagaraja, A. Rao, P.D. Babu and G.S. Okram // *Physica B* **479** (2015) 10.
[71] Y. Jin, X.P. Cui, J.A. Cheng, S.X. Cao, W. Ren and J.C. Zhang // *Applied Physics Letters* **107** (2015) 072907.
[72] H. Nhalil and S. Elizabeth // *J. Supercond. Nov. Magn.* **30** (2017) 1681.
[73] O. Peña, K. Ghanimi, C. Moure, D. Gutiérrez and P. Durán // *Bol. Soc. Esp. Ceram. V.* **43** (2004) 706.
[74] O. Peña, C. Moure, P. Barahona, M. Baibich and G. Martinez // *Physica B* **384** (2006) 57.
[75] R.R. Zhang, G.L. Kuang, L.H. Yin and Y.P. Sun // *J. Alloy. Compd.* **519** (2012) 92.
[76] S. Biswas, M.H. Khan, S. Pal and E. Bose // *J. Magn. Magn. Mater.* **328** (2013) 31.
[77] S. Biswas, M.H. Khan, S. Pal and E. Bose // *J. Supercond. Nov. Magn.* **27** (2014) 463.
[78] A. Modi and N. K. Gaur // *Journal of Alloys and Compounds* **644** (2015) 575.
[79] P. Mandal, C.R. Serrao, E. Suard, V. Caignaert, B. Raveau, A. Sundaresan and C.N.R. Rao // *J. Solid State Chem.* **197** (2013) 408.
[80] M. Mihalik, M. Fitta, M. Balanda, M. Vavra, S. Gabáni, M. Zentková and J. Briancin // *J Magn. Magn. Mater.* **345** (2013) 125.